

Melting and Crystallization Behaviors of Injection-Molded Polypropylene

MITSUYOSHI FUJIYAMA, ISAO MASADA, KATSUO MITANI

Plastics Development Laboratory, Tokuyama Corporation, 1-1, Harumi-cho, Tokuyama-shi, Yamaguchi-ken, 745-0024 Japan

Received June 1999; accepted November 1999

ABSTRACT: The melting and crystallization behaviors of the skin layer in an injection-molded isotactic polypropylene (PP) have been studied, mainly in comparison with those of the core layer and subsidiarily in comparison with those of a compression-molded PP and a nucleator (talc)-added PP. The skin layer contains about 5% crystals, which have a high melting point of up to 184°C. They thermally vanish by melting once. The subsequent melting history will scarcely affect the melting behaviors. On the other hand, crystallization behaviors are strongly affected by the melting history. The skin layer crystallizes in a wide temperature range at high temperature. This tendency weakens with increasing melting temperature, approaching a constant and that of the core layer above 230°C, which suggests that the memory effect of the residual structure of PP vanishes by melting above 230°C. In explaining these experimental results, it is assumed that the residual structure substance is a melt orientation of molecular chains that works as crystallization nuclei and that the vanishing of the residual structure is nothing but a relaxation of the melt orientation. © 2000 John Wiley & Sons, Inc. *J Appl Polym Sci* 78: 1751–1762, 2000

Key words: isotactic polypropylene; injection molding; melting; crystallization; residual structure

INTRODUCTION

It is well known that the crystallization behaviors of a semicrystalline polymer are affected by the melting conditions, and a residual structure remains at temperatures even above the melting point. Majer¹ studied the effect of melting temperature on the isothermal crystallization behaviors of isotactic polypropylene (PP) and found that by changing the melting temperature between 190°C and 220°C, the Avrami's exponent n uniformly increased from 2.4 to 3.4 and the time

during which the crystallization progressed by half, $t_{1/2}$, uniformly increased from 18 min to 23 min. In order to reexamine Majer's results, Yoshizaki et al.² measured the isothermal crystallization behaviors of PP by changing the melting temperature to between 185°C and 215°C. They found that by increasing the melting temperature from 195°C to 205°C, the crystallization rate rapidly decreased to a constant and the Avrami's exponent n increased rapidly from 2 to constant 2.7. They also showed that the crystallization rate of the drawn PP sample that melted at 195°C increased with increasing draw ratio. Ikushima et al.³ studied the effect of melting conditions on the isothermal crystallization behaviors of various grade PPs and found that crystallization rate generally decreased with increasing melting temper-

Correspondence to: M. Fujiyama (m-fujiyama@tokuyama.co.jp).

Journal of Applied Polymer Science, Vol. 78, 1751–1762 (2000)
© 2000 John Wiley & Sons, Inc.

ature. In order to study the effect of thermal and mechanical histories, Michel⁴ melt-mixed PP pellets with a single-screw extruder at 200°C and 255°C. The crystallization rate when melted at 228°C and isothermally crystallized at 128°C was higher for the 200°C-mixture than for the 255°C-mixture, decreased with mixing time, and approached a constant value at about 10 min for the 255°C-mixture and at about 40 min for the 200°C-mixture. They also showed that the crystallization temperature at constant-rate cooling of the 200°C-mixture was about 10°C higher than that of the 255°C-mixture. Fujiyama et al.⁵ investigated the melting and crystallization behaviors of a PP crosslinked with the aid of a liquid polybutadiene and a peroxide. They found that although the crosslinked PP showed a melting point about 10°C lower than noncrosslinked PP, the former showed a crystallization temperature about 15°C higher than the latter and crystallizes in wider temperature range than the latter. They presumed these facts to be true because crosslinked PP has a wide range of strong residual structures at temperatures above the melting point. Rybníkář⁶ measured the dependence of a number of crystallization nuclei of a PP and a 10 wt % talc-filled PP on the melting temperature. They showed that there exist two types of crystallization nuclei: (1) a metastable nucleus consisting of an unmelted PP crystal phase stabilized by solid impurities, which exists in cases of low melting temperature and short melting time and (2) a stable one consisting of solid impurities that are assumed perhaps to be catalyst residues. The total number of nuclei is about 2 decades more for the talc-filled PP than for the PP. The number of metastable nuclei rapidly decreases with increasing melting temperature, approaches a constant value at about 210°C for the PP and at about 225°C for the talc-filled PP, and only stable nuclei remain.

The authors⁷ have previously studied the crystalline structure of injection-molded PP by means of wide-angle X-ray diffraction, small-angle X-ray scattering, melting behavior, density, dynamic viscoelasticity, and tensile test. They had assumed that the skin layer consists of a crystalline structure such as that shown in Figure 1 and the core layer consists of the usual spherulites. The skin layer is composed of shish-kebab-like main skeleton structure, whose axis is parallel to the flow direction, piled epitaxially with an a^* -axis-oriented imperfect lamellar substructure. The

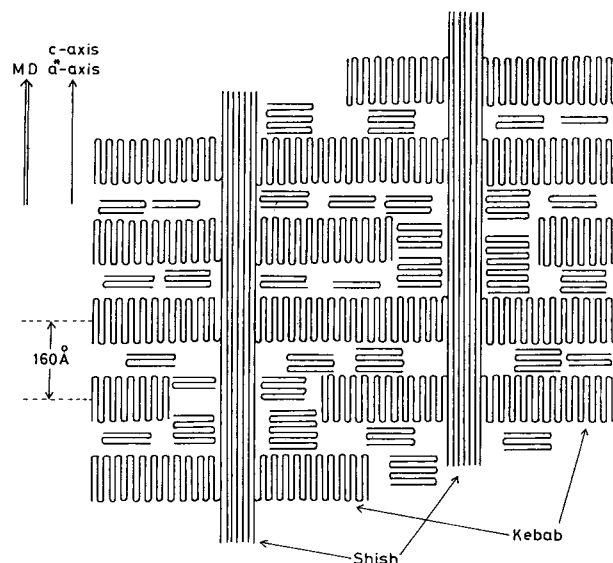


Figure 1 Schematic representation of crystalline structure of skin layer in injection-molded polypropylene.

skin layer has crystalline parts showing a high melting temperature of up to 182°C because of the existence of about 5% shish crystals. The existence of a high-temperature melting component of the injection-molded semicrystalline polymers has been observed in the surface layer of the usual injection-molded high-density polyethylene (HDPE)⁸ and in self-reinforced HDPE^{9–20} and PP^{13,20–23} prepared by low-temperature and high-pressure injection molding,^{9–15,21} by elongational flow injection molding,¹⁶ and by vibration injection molding.^{17–20,22,23} It has been reported that the high-temperature melting component vanishes by heating the sample to a temperature above the melting point.⁹ Varga²¹ studied the effect of melting conditions on the crystallization behaviors of self-reinforced PP prepared by low-temperature and high-pressure injection molding and found that the crystallization rate and the temperature range of crystallization at a constant-rate cooling are higher and wider, respectively, when the melting temperature (175°C–200°C) is nearer the melting point. At the same time, using polarized microscopy, he showed that a fibrillar component with a birefringence remains even after melting at low temperatures below 190°C, and that a crystalline texture similar to the original one reappears with recrystallization.

In the present article we report on our study of the melting and crystallization behaviors of the

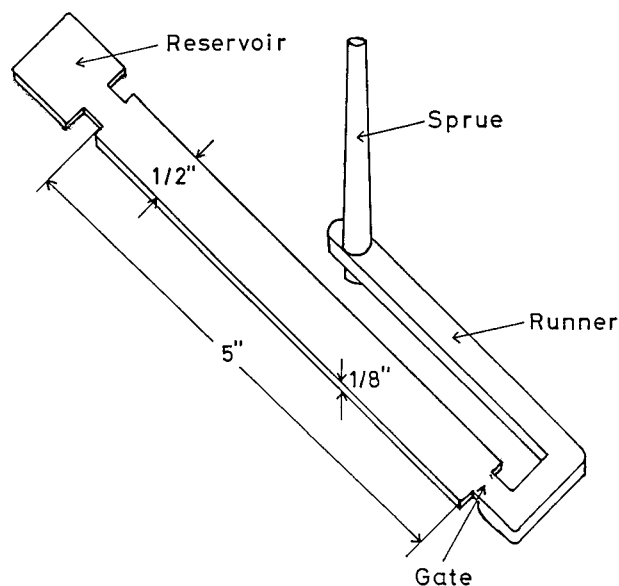


Figure 2 Shape of test specimen.

skin and core layers in an injection-molded PP, compared with those of a compression-molded PP and a crystallization nucleator-added PP. The current study has added new information and considerations, which are briefly reported in this article.

EXPERIMENTAL

Samples

A homoisotactic polypropylene (PP) with an MFI of 1.6 g/10 min, produced by the Tokuyama Corp., Japan, was used. Used for the crystallization nucleator was a talc (micron white #5000S, produced by the Chem Hayashi Company, Japan) with an average particle size of 2.8 μm .

Specimen Preparation

Flexural test specimens (ASTM D790), shown in Figure 2, were injection-molded from the PP by using an 8-oz reciprocating-screw injection-molding machine (Nikko Ankerwrk V22A-120, Japan). Although the injection molding was carried out under various molding conditions, the specimens actually used in the experiment were those with the clearest skin-core structure, which were molded under the following conditions:

cylinder temperature: $C_1 = 160^\circ\text{C}$, $C_2 = 190^\circ\text{C}$,
 $C_3 = 200^\circ\text{C}$, $N = 190^\circ\text{C}$
 injection pressure: 30 MPa
 injection rate: 33 cm^3/s
 mold temperature: 40°C
 cooling time: 10 s

These are the same molding conditions as those for the specimens reported on in the previous article.⁷

The thickness of the skin layer of the flexural specimen in this experiment was about 0.6 mm, as shown in Figure 3. The skin (IM-S) and core layer (IM-C) specimens, of about 0.3 mm thickness, were sliced from, respectively, the surface and the center of the central part of the flexural specimen parallel to its surface, as shown in Figure 4.

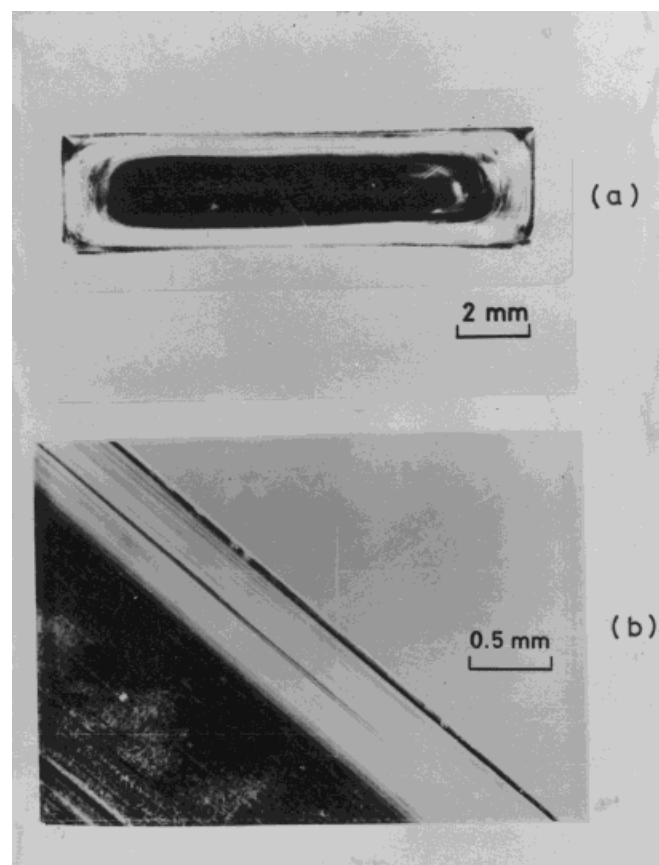


Figure 3 (a) Polarized micrograph of thin section of injection-molded polypropylene cut perpendicular to flow direction under crossed polars; (b) Enlarged photograph of (a).

Flexural Test Specimen (ASTM D790)

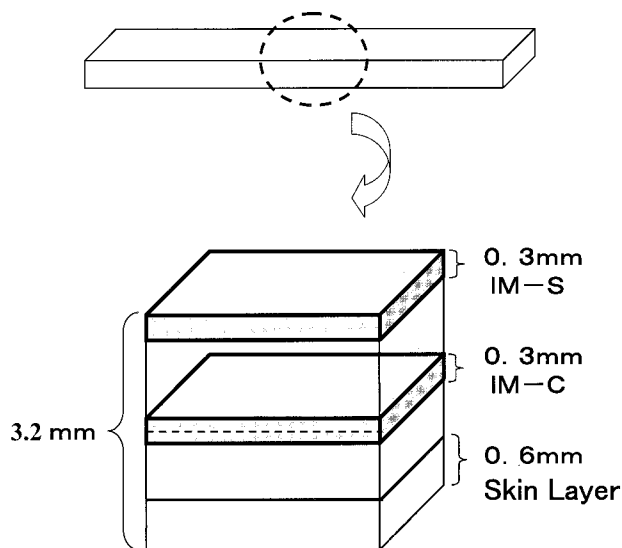


Figure 4 Schematic representation of specimen preparation.

The compression-molded specimen (CM) was obtained by melting PP pellets between two slide glasses on a hot plate at 200°C for 5 min, pressing with a pincette to about 0.3 mm thickness, and then cooling in ambient air.

A PP powder containing the same amount of such additives as thermal stabilizers as the PP pellets did was thoroughly mixed with 0.5 wt % talc as crystallization nucleator and melt-mixed in a Brabender Plastograph (Germany) at 200°C for 5 min, followed by cooling in ambient air. A small amount of the mixture was compression-molded in the same manner as the CM specimen, creating the nucleated PP specimen (N-PP).

Measurement of Melting and Crystallization Behaviors

The melting and crystallization behaviors were measured using the Perkin-Elmer differential scanning calorimeter DSC-IB (USA). The DSC had been calibrated by indium for temperature and enthalpy correction. A circular specimen weighing about 10 mg was cut from the sheet specimen and put into a sample pan. The melting thermogram was measured by raising the temperature from 90°C to a maximum melting temperature (MMT) at a rate of 10°C/min. As soon as the temperature reached the MMT, it was cooled

to 90°C at a rate of 10°C/min, and the crystallization thermogram was measured. When the temperature reached 90°C, the second and third runs of melting and crystallization were measured in the same conditions as the first run had been, as shown in Figure 5. As the maximum melting temperature (MMT), 190°C, 210°C, 230°C, and 250°C were selected. The second and the third runs were carried out only for the IM-S specimen, and only the first run was carried out for the other specimens. These measurements were carried out in a nitrogen atmosphere.

All thermograms were normalized on a same-sample weight.

EXPERIMENTAL

Melting Behavior

Figure 3 shows polarized micrographs of a thin section, about 0.1 mm thick, cut perpendicular to the flow direction (MD) at the central part of the injection-molded specimen. Since these photographs were printed with a quick copier, light and darkness are inverted. Figure 3(a) shows that the injection-molded specimen has a clear two-phase structure of skin and core. Figure 3(b), which is an enlarged photograph of Figure 3(a), shows that the skin layer is composed of a textureless oriented crystal at this magnification and that the core layer is composed of spherulites.

Figure 6 shows melting thermograms for the first melting of the original samples. Each sample begins an endotherm from about 120°C and shows a peak at 163°C–167°C. Although the core layer specimen (IM-C) and the compression-molded specimen (CM) end melting at about

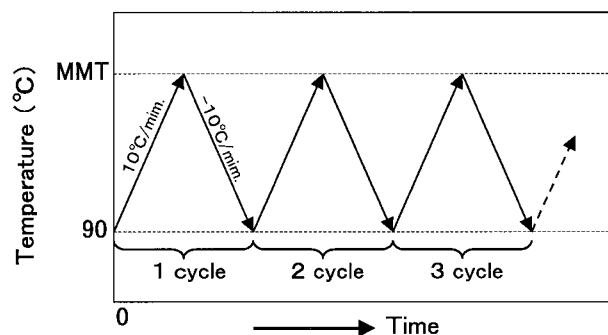


Figure 5 Temperature profile program of DSC measurement.

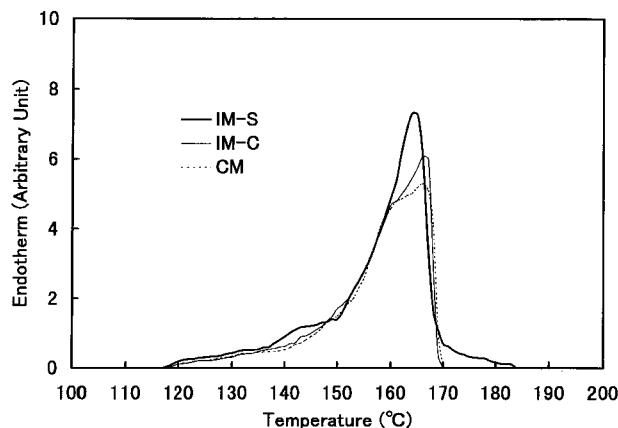


Figure 6 Melting thermograms for first melting of original specimens.

170°C, the skin layer specimen (IM-S) has crystals with a melting point up to 184°C. The area fraction of the high-temperature (above 170°C) melting component is about 5%. The crystals with high melting temperature are shish crystals, shown in Figure 1.⁷ The melting behavior of the IM-C is similar to that of the CM.

Figure 7 compares first- and second-time melting thermograms of the IM-S. By melt-recrystallization, although the peak temperature (T_{mp}) slightly decreases, the high-temperature melting component vanishes and the melting-end temperature (T_{me}) largely decreases. Because the high-temperature melting component vanishes by melting at a low temperature of 190°C, higher than the T_{me} by only 6°C, it can be assumed that the shish crystals are thermally unstable and the

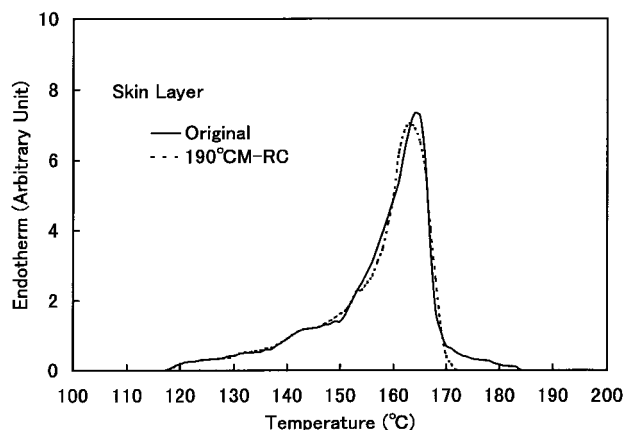


Figure 7 Melting thermograms for first- and second-time melting of skin layer.

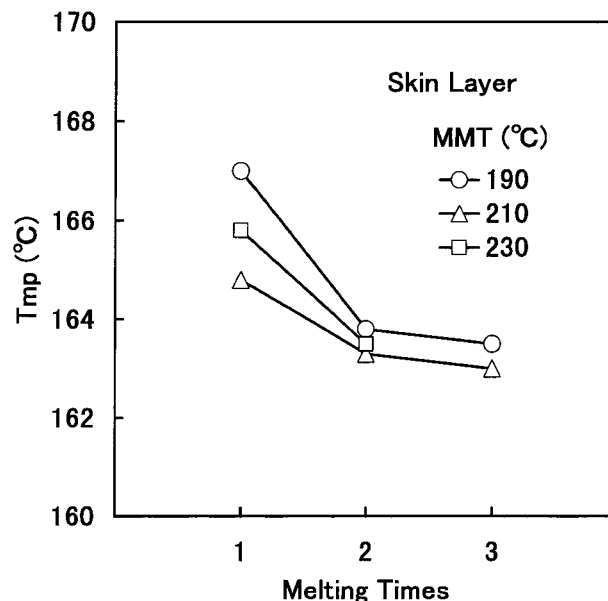


Figure 8 Dependence of melting peak temperature (T_{mp}) on melting time.

crystal chain stretching disorders in a short time at temperatures above the melting point; by recrystallization, although a sign of the nucleus may remain, fibrillar recrystallization must not occur.

Figure 8 shows the dependence of the T_{mp} of the IM-S on melting time. Although data show some scattering, T_{mp} lowers by 2°C–3°C by the first melting and scarcely changes from the following melting. It seems that the effect of maximum melting temperature (MMT) is slight. Figure 9 shows the dependence of the T_{me} of the IM-S on melting time. A T_{me} above 180°C for the original specimen lowers by about 10°C from the first melting and seems to scarcely change after that. The effect of the MMT is slight. Figure 10 shows the dependence of heat of fusion, ΔH_m , of the IM-S on melting time. ΔH_m decreases by about 10% by the first melting and scarcely changes after that.

From above, it may be said that when the skin layer of injection molding is melt-recrystallized once it becomes stable in melting behavior and is scarcely affected by the previous melting history. However, the crystallization behavior is strongly affected by the previous melting history, as shown below.

Crystallization Behavior

Figure 11 shows a comparison of crystallization thermograms after the first melting at an MMT of

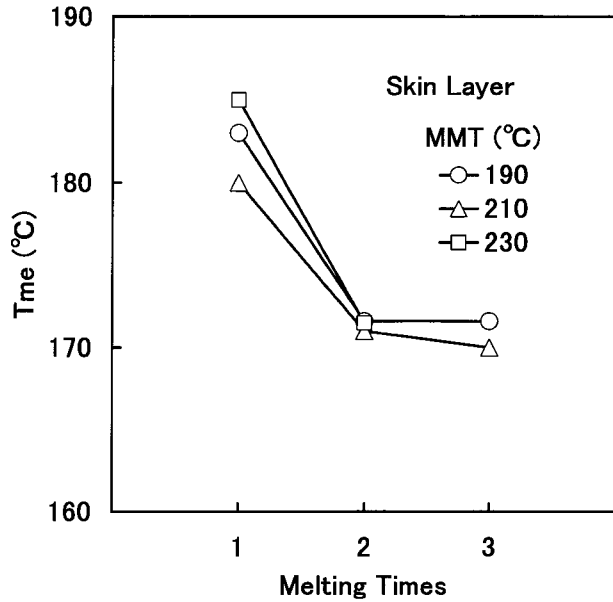


Figure 9 Dependence of melting-end temperature (T_{me}) on melting time.

190 °C. At first, the IM-S and IM-C are compared. The IM-S begins crystallization at a higher temperature, crystallizes in a wider temperature range, shows a peak at a higher temperature than the IM-C, while the crystallization-end temperature is nearly the same for both the samples. The

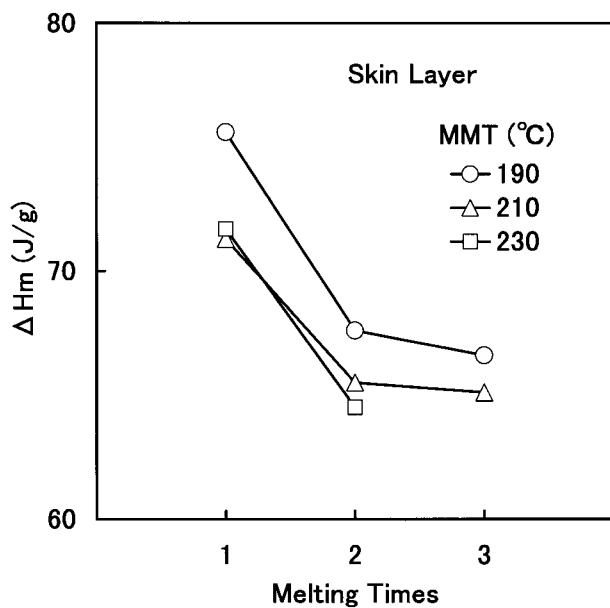


Figure 10 Dependence of heat of fusion, ΔH_m , on melting time.

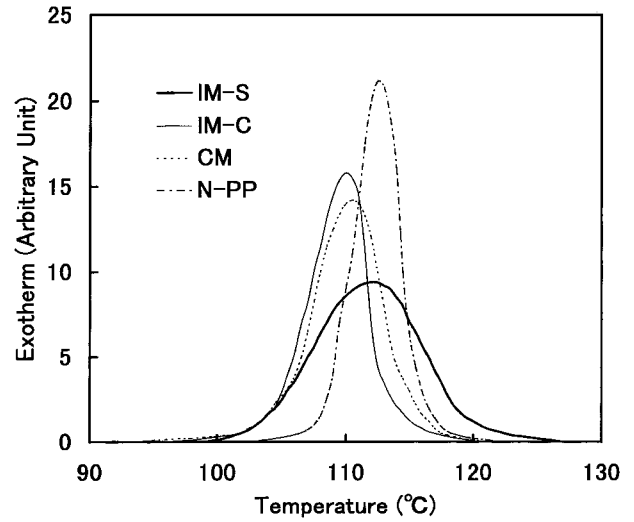


Figure 11 Crystallization thermograms after first melting at 190 °C.

CM shows a similar crystallization behavior to the IM-C. Although the N-PP shows a higher crystallization peak temperature than the IM-S, it begins crystallization from a lower temperature, ends crystallization at a higher temperature, and crystallizes in a narrower temperature range than the IM-S. The width of the crystallization temperature of the N-PP is narrower than those of the IM-C and CM.

Figure 12 shows the dependence of the crystal-

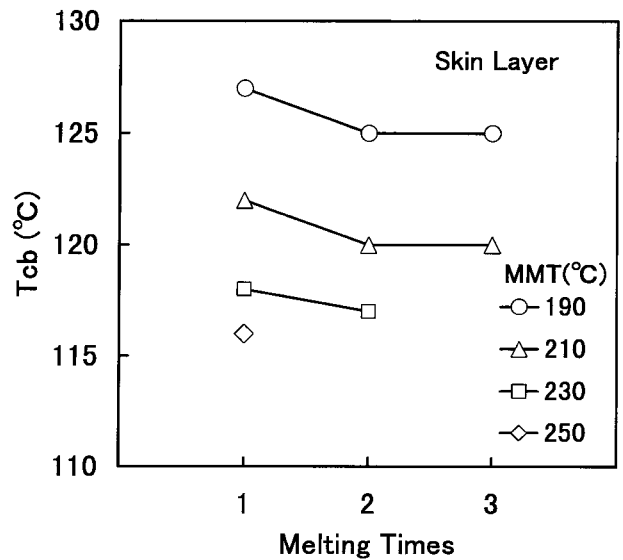


Figure 12 Dependence of crystallization-beginning temperature (T_{cb}) on melting time.

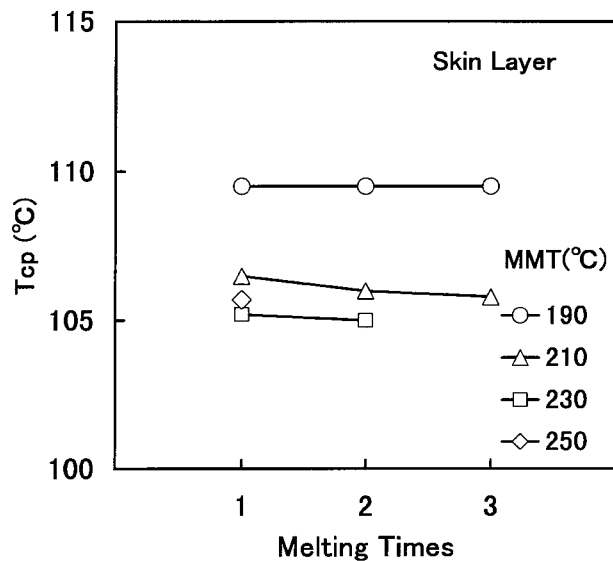


Figure 13 Dependence of crystallization peak temperature (T_{cp}) on melting time.

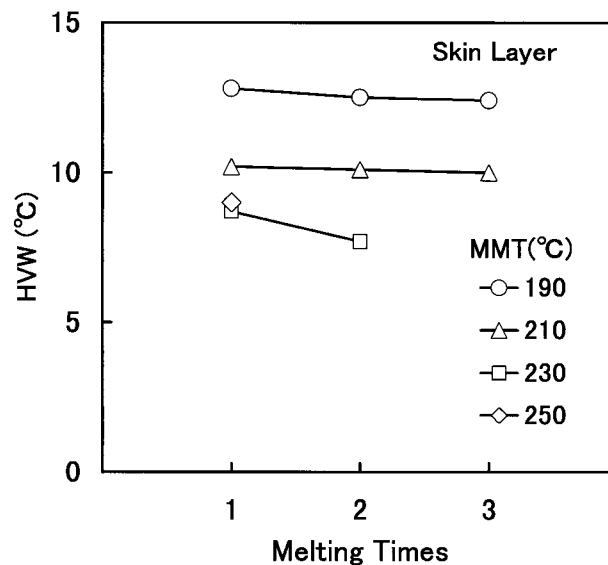


Figure 14 Dependence of half-value width of crystallization peak, HVW, on melting time.

lization-beginning temperature (T_{cb}) of the IM-S on melting time. The T_{cb} lowers by 1°C–2°C from the first to second melting and scarcely changes after that. The effect of the MMT is more prominent than that of melting time, and a lower MMT leads to a higher T_{cb} . Figure 13 shows the dependence of the crystallization peak temperature (T_{cp}) of the IM-S on melting time. The T_{cp} tends to lower slightly with increasing melting time. T_{cp} tends to rise with a decreasing MMT. Figure 14 shows the dependence of the half-value width of crystallization peak, HVW, of the IM-S on melting time. The HVW tends to decrease slightly with increasing melting time. It also tends to increase with a decreasing MMT. Figure 15 shows the dependence of latent heat of crystallization, ΔH_c , of the IM-S on melting time. The ΔH_c scarcely depends on melting time and shows a maximum at an MMT of 210°C.

Figure 16 shows the dependence of the T_{cb} after the first melting on the MMT. The T_{cb} of each sample tends to decrease with the MMT. This decrease is particularly notable for the IM-S at MMTs below 230°C. The T_{cb} 's of the IM-S and IM-C are nearly the same at MMTs above 230°C. The order of the T_{cb} at low MMTs is IM-S > IM-C \approx N-PP > CM.

Figure 17 shows the dependence of the T_{cp} after the first melting on the MMT. The T_{cp} tends to slightly lower with the MMT at MMTs below 230°C. The T_{cp} of the IM-S is nearly the same as

those of the IM-C and CM at MMTs above 210°C. The order of the T_{cp} at an MMT of 190°C is N-PP > IM-S > CM > IM-C.

Figure 18 shows the dependence of the HVW after the first melting on the MMT. The HVW of the IM-S decreases with an increasing MMT and tends to level off above 230°C, while it may be

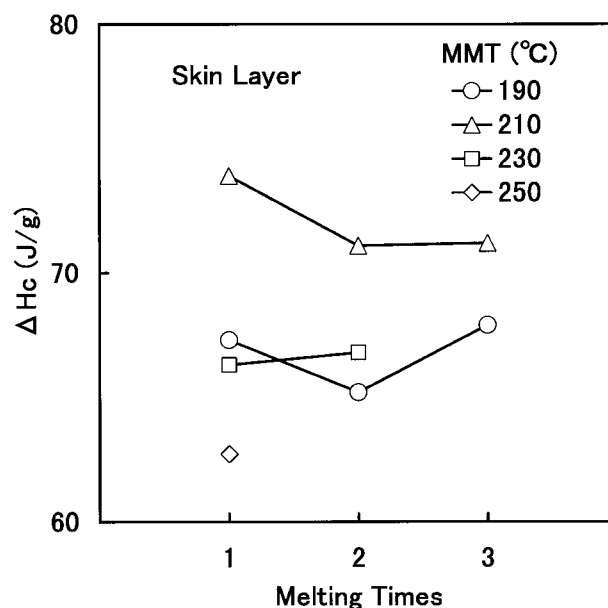


Figure 15 Dependence of latent heat of crystallization, ΔH_c , on melting time.

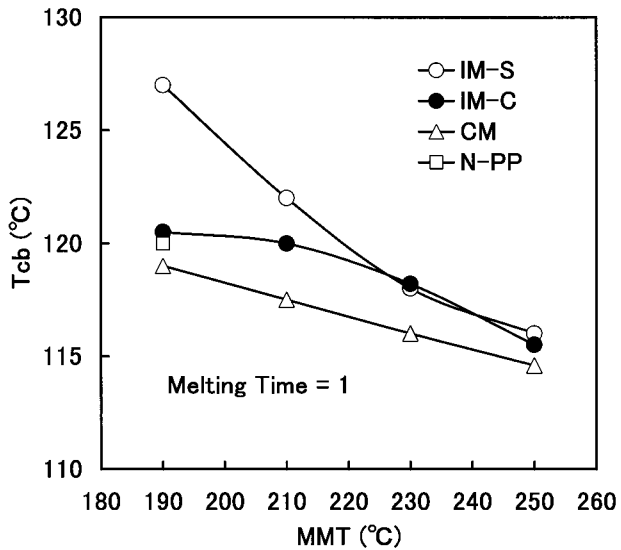


Figure 16 Dependence of crystallization-beginning temperature (T_{cb}) after first melting on maximum melting temperature (MMT).

regarded that the HVWs of the IM-C and CM do not depend so much on the MMT. Although the HVW of the IM-S is larger than that of the IM-C at all MMTs, the difference between them decreases with an elevating MMT, and the former comes near the latter at MMTs above 230°C. The order of the HVW at an MMT of 190°C is IM-S > CM > IM-C > N-PP.

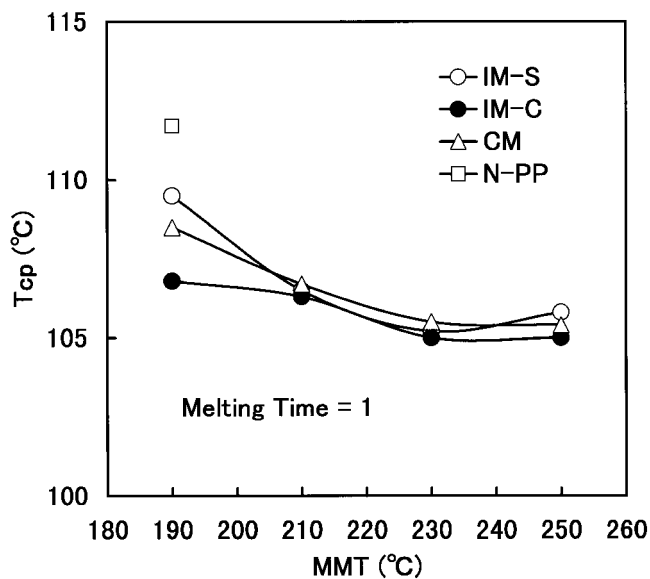


Figure 17 Dependence of crystallization peak temperature (T_{cp}) after first melting on maximum melting temperature (MMT).

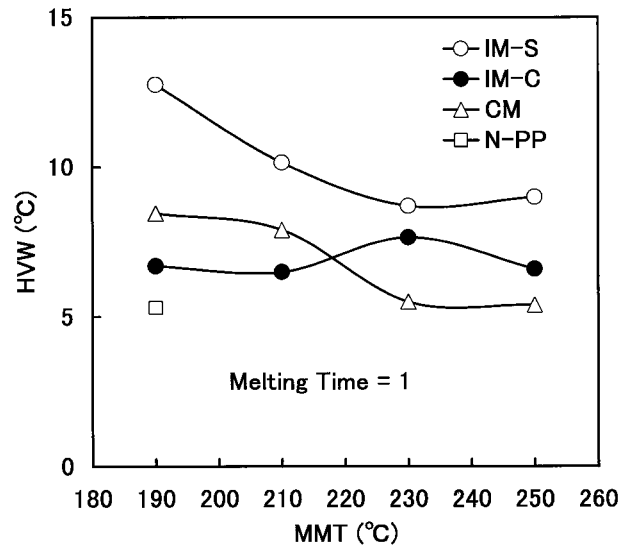


Figure 18 Dependence of half-value width of crystallization peak, HVW, after first melting on maximum melting temperature, MMT.

Figure 19 shows the dependence of the ΔH_c after the first melting on the MMT. The ΔH_c of each sample tends to show a maximum at an MMT of 200°C–210°C. The order of the ΔH_c at an MMT of 190°C is N-PP > CM > IM-C \approx IM-S.

DISCUSSION

The experimental results on melting and crystallization behaviors of an injection-molded PP are

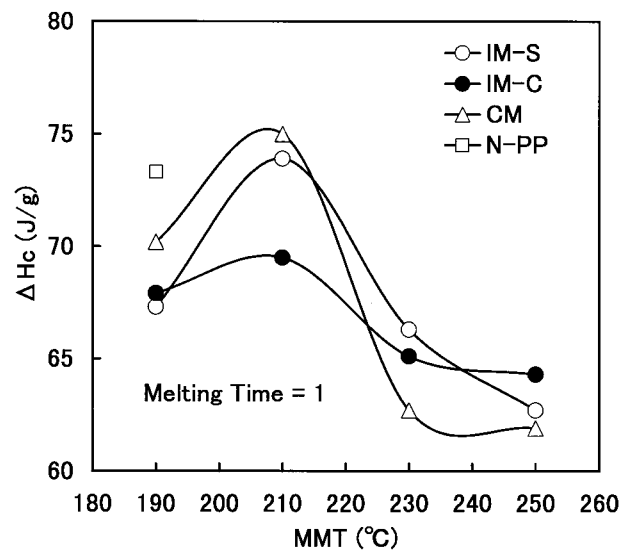


Figure 19 Dependence of latent heat of crystallization, ΔH_c , after first melting on maximum melting temperature, MMT.

summarized centering around the skin layer as follows:

1. The skin layer has about 5% crystals, with a high melting point of up to 184°C, which thermally vanish by melting once and do not appear at the following recrystallization. The melting-end temperature of the skin layer scarcely changes from the second-time melting and becomes similar to those of the core layer and compression-molded specimen. The melting peak temperature lowers by 2°C–3°C by the first melting, and the following melting history scarcely affects it.
2. The skin layer recrystallizes in a wide temperature range at high temperatures. The crystallization-beginning temperature (T_{cb}) and the crystallization peak temperature (T_{cp}) of the skin layer lower with increasing maximum melting temperature (MMT) and approach those of the core layer above 230°C and 210°C, respectively. Although the T_{cb} of nucleator (talc)-added PP is lower than that of the skin layer, the T_{cp} of the former is higher than that of the latter.
3. The half-value width of crystallization peak, HVW, of the skin layer is larger than those of the core layer and compression-molded specimen and approaches a constant and that of the core layer at MMTs above 230°C. The HVW of the nucleator-added PP is narrower than that of the core layer.
4. The latent heat of crystallization of each sample shows a maximum at an MMT of 200°C–210°C.

Because the high-temperature melting crystals in the skin layer vanish by melting once at a temperature slightly higher than the melting point, it may be said that the skin layer becomes stable in melting behavior by one-time melting and recrystallization. However, because the crystallization behavior is largely affected by the melting history, as explained in points 2–4 above, it can be assumed that the skin layer is unstable in crystallization behavior at melting temperatures below 230°C and that some residual structure which does not affect the melting behavior but the crystallization behavior, exists. This feature is particularly notable for the skin layer. Since this residual structure does not affect the

melting behavior, it must not be clear crystal but some substance capable of becoming a crystallization nucleus. Particularly notable is the residual structure in the skin layer at low melting temperatures, approaching that of the core layer at melting temperatures above 230°C. This may be regarded as the melt orientation of molecular chains existing even in molten state. The structural difference between the skin layer and the core layer and compression-molded specimen is in crystal orientation. That the recrystallization rate of drawn PP increases with the draw ratio, as shown by Yoshizaki et al.,² also supports the assumption that the melt orientation acts as a crystallization nucleus. The dependence of the crystallization behavior of the skin layer on the MMT shows a tendency similar to the results of the experiments by Varga,²¹ which were carried out in a melting temperature range of 175°C–200°C. With both results, crystallization behaviors depend on the melting temperature, approaches a constant at high melting temperatures. The only difference is that in Varga's experimental results, that temperature is above about 200°C, while in the present experiment it approached a constant at melting temperatures above about 230°C. It is assumed that the crystalline structure of the skin layer of conventional injection molding is similar to that of self-reinforced injection molding prepared by low-temperature and high-pressure injection molding²²; hence, the melting and crystallization behaviors of both are also similar. The difference in temperatures above which the dependence of recrystallization behaviors approaches a constant between Varga's and the present experiments is about 30°C, which is about the same as the difference in the resin temperatures of the injection moldings used in both experiments: about 180°C for Varga's experiments and about 210°C (maximum cylinder temperature of 200°C) in the present experiments. It is assumed that the resin temperature at injection molding affects the subsequent recrystallization behaviors of the molding.

That the recrystallization behaviors of the skin layer approach those of the core layer and of compression-molded PP and that they become stable above about 230°C suggests that the skin layer recrystallizes to spherulites after melting above about 230°C.

It is believed that when a specimen with molecular orientation is melted, an oriented state with low entropy is relaxed and deformed to a

random-coil state with high entropy. At this time, since the deformation is affected not only by the conformation of molecular chains themselves but also by the environment such as the entanglement of molecular chains, the relaxation of molecular orientation does not occur instantaneously but takes some time. According to the tube model of de Gennes²⁴ and Doi-Edwards,²⁵ a molten molecular chain can not move freely but is constrained by an imaginary tube formed by environmental molecular chains and only reptation motion along the tube is permitted. If the molecular chain is oriented, it must move out from an oriented tube by reptation in order to relax, and a long time is needed for the chain to relax.

It is also assumed that the residual melt orientation is more prominent the more the initial orientation is higher, its relaxation time is longer, and the time until recrystallization is shorter. As shown in Figure 1, the skin layer is composed of various crystalline structures with different degrees of molecular orientation, such as the fibrous shish crystals, the tie molecule crystals connecting the kebab crystals, the kebab crystals composed of lamellae with thickness distribution, and the imperfect and small a^* -axis-oriented crystals. Accordingly, when the skin layer is melted, melt orientations of various degrees appear. Since they have different crystallization nucleating effects, the recrystallization is assumed to occur in a wide temperature range, which explains the experimental results of high crystallization beginning temperature (T_{cb}) and large half-value width of crystallization peak (HVW). That the T_{cb} and HVW of the skin layer are higher as the melting temperature lowers results from the longer relaxation time of melt orientation and that crystallization occurs sooner, causing less relaxation and more of the melt orientation remaining at recrystallization. The dependence of the T_{cb} on melting time is weaker compared to its dependence on melting temperature because of a long relaxation time and its strong temperature dependence: The relaxation time of melt orientation is longer than that of stress,²⁶ and its temperature dependence obeys the Arrhenius equation. Although the T_{cb} rapidly lowers with an increasing MMT, as shown in Figures 14 and 15, the T_{cp} scarcely changes with the MMT, suggesting that the relaxation and the collapse of the melt-oriented nuclei occur preferentially from the one with higher degree of orientation. According to this theory, for which experimental examination has not been done, an

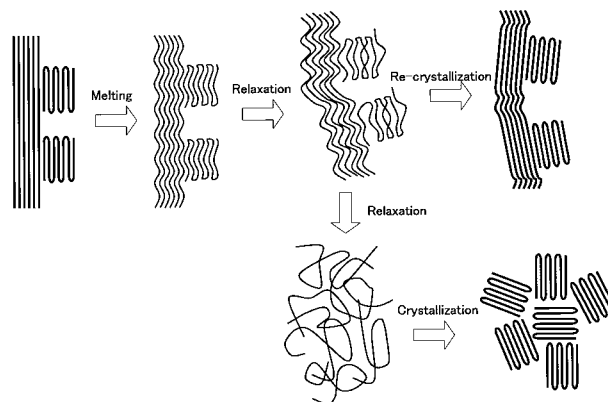


Figure 20 Schematic model of melt-recrystallization of skin layer.

injection molding with a higher molecular weight should show a more prominent residual structure effect from a higher initial orientation and longer relaxation time. Furthermore, a crosslinked PP, similar to the skin layer of injection-molded PP, crystallizes in a wide temperature range at high temperatures during melt-recrystallization (for a complete analysis, see the Introduction section). This is because, since molecular chains are fixed with crosslinking points in crosslinked PP, the structural distribution is wide, leading to a long relaxation time of the residual structure (molecular orientation) and a wide distribution of the relaxation time in the molten state. From the viewpoint of wide distribution of the residual structure in molten state, the crosslinked PP is similar to the skin layer of injection-molded PP, with the former perhaps more prominent than the latter. A schematic model of melt-recrystallization of skin layer is represented in Figure 20.

The high crystallization temperature of the nucleator-added PP originates from the progress in crystallization using talc working as nuclei, which differs from the melt orientation. Of course, the crystallization by the nuclei of residual structures of crystal orientation is assumed to coexist. An explanation of the present theory according to Rybníkář⁶ is that the melt orientation corresponds to the metastable nucleus of Rybníkář and the talc corresponds to the stable nucleus. The crystallization of nucleator-added PP occurs mainly with the impurities working as nuclei; hence, the range of crystallization temperatures is narrow and the HVW is small.

And, finally, we would like to discuss the phenomenon of the latent heat of crystallization

showing a maximum at around 210°C. The lower melting temperature is assumed to cause more residual structures, leading to easier crystallization with them working as nuclei and hence to higher crystallinity. Meanwhile, the lower melting temperature is assumed to cause more residual structures with low entropy, leading to crystallization with smaller change of entropy and hence with lower exothermic heat. It is assumed that when an increase in crystallinity and a decrease in crystallization entropy are balanced, the maximum of latent heat of crystallization will appear at around 210°C.

CONCLUSIONS

The melting and crystallization behaviors of the skin and core layers in an injection-molded PP were studied and compared with those of compression-molded PP and crystallization nucleator-added PP, producing the following results:

1. The skin layer has about 5% crystals, which have a high melting point of up to 184°C. They thermally vanish by melting once and do not appear at the following recrystallization. The melting-end temperature of the skin layer scarcely changes from the second-time melting and becomes similar to those of the core layer and compression-molded specimen. The melting peak temperature lowers by 2°C–3°C by the first melting, and the following melting history scarcely affects it.
2. The skin layer recrystallizes at high temperature in a wide temperature range. The crystallization-beginning temperature (T_{cb}) and the crystallization peak temperature (T_{cp}) of the skin layer lower with increasing maximum melting temperature (MMT) and approach those of the core layer above 230°C and 210°C, respectively. Although the T_{cb} of nucleator (talc)-added PP is lower than that of the skin layer, the T_{cp} of the former is higher than that of the latter.
3. The half-value width of crystallization peak, HVW, of the skin layer is larger than those of the core layer and compression-molded specimen and approaches a constant and that of the core layer at MMTs above 230°C. The HVW of the nucleator-

added PP is narrower than that of the core layer.

4. The latent heat of crystallization of each sample shows a maximum at an MMT of 200°C–210°C.

The explanation for these experimental results assumes that the substance of the residual structure is a melt orientation of molecular chains that works as crystallization nuclei and that the vanishing of the residual structure is nothing but a relaxation of the melt orientation. Since the skin layer shows a high degree of molecular orientation and is composed of various crystals with different degrees of orientation, the degree of melt orientation is also high and its distribution also wide when melted, leading to recrystallization in a wide temperature range at high temperature. The effect of melting history weakens with increasing melting temperature because the relaxation of melt orientation becomes easier. Because the dependence of crystallization behaviors on the melting temperature of the skin layer vanishes at temperatures above 230°C and approaches those of the core layer and compression-molded PP, it is assumed that the residual structure in the melt of PP vanishes above 230°C. It is also supposed that the skin layer recrystallizes to spherulites after melting above 230°C.

The authors would like to thank Tokuyama Corp. for permission to publish this article.

REFERENCES

1. Majer, J. *Kunststoffe* 1960, 50, 565.
2. Yoshizaki, O.; Ishibashi, T.; Nagai, E. *Kogyo Kagaku Zasshi* 1962, 65, 1614.
3. Ikushima, K.; Tanaka, T.; Nomoto, H. *Kobunshi Ronbunshu* 1972, 29, 186.
4. Michel, J. C. *SPE Tech Paper*, 52nd ANTEC 1994, 40, 2266.
5. Fujiyama, M.; Koya, Y.; Azuma, K. *Kobunshi Ronbunshu* 1980, 37, 797.
6. Rybníkář, F. *J Appl Polym Sci* 1982, 27, 1479.
7. Fujiyama, M.; Wakino, T.; Kawasaki, Y. *J Appl Polym Sci* 1988, 35, 29.
8. Tan, V.; Kamal, M. R. *J Appl Polym Sci* 1978, 22, 2341.
9. Djurner, K.; Kubát, J.; Rigdahl, M. *J Appl Polym Sci* 1977, 21, 295.
10. Kubát, J.; Månson, J.-A. *Polym Eng Sci* 1983, 23, 869.

11. Kubát, J.; Månson, J.-A.; Rigdahl, M. *Polym Eng Sci* 1983, 23, 877.
12. Ehrenstein, G. W.; Maertin, C. *Kunststoffe* 1985, 75, 105.
13. Maertin, C.; Ehrenstein, G. W. *SPE Tech Paper*, 45th ANTEC 1987, 33, 816.
14. Boldizar, A.; Jacobsson, S.; Hård, S. *J Appl Polym Sci* 1988, 36, 1567.
15. Boldizar, A.; Kubát, J.; Rigdahl, M. *J Appl Polym Sci* 1990, 39, 63.
16. Dueda, D. R.; Bayer, R. K.; Baltá Calleja, F. J. *J Macromol Sci, Phys* 1989, B28, 267.
17. Ogbonne, C. I.; Kalay, G.; Allan, P. S.; Bevis, M. J. *J Appl Polym Sci* 1995, 58, 2131.
18. Guan, Q.; Shen, K.; Ji, J.; Zhu, J. *J Appl Polym Sci* 1995, 55, 1797.
19. Guan, Q.; Lai, F. S.; McCarthy, S. P.; Chiu, D.; Zhu, X.; Shen, K. *Polymer* 1997, 38, 5251.
20. Ibar, J. P. *Polym Eng Sci* 1998, 38, 1.
21. Varga, J. *Magy Kém Foly* 1989, 95, 416.
22. Kalay, G.; Bevis, M. J. *J Polym Sci, Phys.* 1997, 35, 265.
23. Guan, Q.; Zhu, X.; Chiu, D.; Shen, K.; Lai, F. S.; McCarthy, S. P. *J Appl Polym Sci* 1996, 62, 755.
24. de Gennes, P. G. *J Chem Phys* 1971, 55, 572.
25. Doi, M.; Edwards, S. F. *J Chem Soc Faraday Trans II* 1978, 74, 1789.
26. Mills, N. J. *Eur Polym J* 1969, 5, 675.